Journal of Applied Pharmaceutical Research
Volume 14 Issue 4, Year of Publication 2026, Page 237 – 246
DOI: https://doi.org/10.69857/joapr.v14i4.2125

Check for updates

Research Article

JOURNAL OF APPLIED PHARMACEUTICAL RESEARCH | JOAPR
www.japtronline.com ***ISSN: 2348 – 0335***

SYNTHESIS, SPECTRAL CHARACTERIZATION, AND IN VITRO ANTICANCER EVALUATION OF NOVEL FLAVANONE-ARYLHYDRAZONE DERIVATIVES

Reena Singh, Yogesh Murti*

Article Information
Received: 6th March 2026
Revised: 12th May 2026
Accepted: 3rd June 2026
Published: 31st July 2026

Keywords
Flavanone, Hydrazone, Breast cancer, MCF-7, MDA-MB-231

ABSTRACT

Background: Flavanones are naturally occurring scaffolds with diverse pharmacological activities, including anticancer potential. Structural modification through hydrazone incorporation may enhance their biological properties and support the development of new therapeutic leads for breast cancer. **Methodology:** A series of nine flavanone-arylhydrazone derivatives was synthesized via condensation of substituted flavanones with phenylhydrazines under reflux conditions. The structures were confirmed using IR, ^{1}H NMR, and high-resolution mass spectrometry (HRMS). The compounds were evaluated for in vitro cytotoxicity against MCF-7 and MDA-MB-231 breast cancer cell lines using the MTT assay, with tamoxifen as the reference drug. **Results and Discussion:** All synthesized compounds exhibited dose-dependent cytotoxicity. Derivatives bearing electron-withdrawing substituents, such as nitro and halogen groups, showed relatively enhanced activity. Compounds 3 and 1 demonstrated the lowest IC_{50} values (33–44 µM), indicating comparatively higher potency within the series. However, only modest differences in activity were observed among derivatives, suggesting that electronic effects alone do not fully govern cytotoxicity. **Conclusion:** Flavanone-arylhydrazone hybrids represent a promising scaffold for anticancer drug development. While electron-withdrawing substituents contribute to activity, the overall structure–activity relationship appears to be influenced by multiple physicochemical factors. Further mechanistic and in vivo studies are required to establish their therapeutic potential.

INTRODUCTION

Flavanones are an important class of flavonoids widely recognized for their diverse pharmacological activities, including antioxidant, anti-inflammatory, and anticancer effects. Their core 2-phenylchroman-4-one structure provides a versatile scaffold for chemical modification[1]. However, naturally occurring flavanones often exhibit moderate biological activity and limited pharmacokinetic properties, which restrict their therapeutic application and necessitate structural optimization[2]. Hydrazone derivatives have gained significant attention in medicinal chemistry due to the presence of the azomethine (–C=N–NH–) functional group, which contributes to a wide range of biological activities, including anticancer potential[3]. These compounds are known to act through

*Institute of Pharmaceutical Research, GLA University, Mathura, Uttar Pradesh, India.

For Correspondence: **ymurti@gmail.com**

mechanisms such as enzyme inhibition, modulation of reactive oxygen species, and interactions with cellular macromolecules [4]. Their structural flexibility and hydrogen-bonding capability make them promising pharmacophores for drug design[5]. Molecular hybridization, which combines two bioactive scaffolds into a single molecular framework, has emerged as an effective approach to enhance biological activity[6]. In this context, incorporating hydrazone moieties into the flavanone scaffold is expected to improve anticancer potential by modulating electronic properties and enhancing molecular interactions with biological targets[7]. Previous studies suggest that substitution with electron-withdrawing groups, such as nitro and halogen substituents, can influence cytotoxic activity by affecting lipophilicity and electronic distribution[8].

Breast cancer remains one of the most prevalent malignancies worldwide, with both hormone-dependent and triple-negative subtypes posing significant therapeutic challenges. Therefore, the development of novel compounds with improved efficacy is of considerable interest[9].

In the present study, a series of novel flavanone–arylhydrazone derivatives were synthesized via condensation reactions and characterized using spectroscopic techniques, including IR, ^{1}H NMR, and mass spectrometry[10]. The synthesized compounds were further evaluated for in vitro anticancer activity against MCF-7 and MDA-MB-231 breast cancer cell lines using the MTT assay to assess their potential as lead candidates for further development [11].

MATERIAL AND METHOD

Chemicals and instrumentation

All of the chemicals and reagents used in this investigation were from approved vendors, including Merck, Sigma-Aldrich, Loba Chemie, Central Drug House (CDH) Pvt. Ltd. (India), and Fischer Scientific (India). They were utilized without any additional purification. Melting points are presented uncorrected and were tested using the open capillary method. On glass plates covered with silica gel G, thin-layer chromatography (TLC) was performed using a mobile phase consisting of ethyl acetate, formic acid, and water (8:1:1). To visualize spots, iodine vapor was used. Using a Bruker Avance 500 MHz spectrometer, proton (^1H) and carbon (^13C) nuclear magnetic resonance (NMR) spectra were acquired in $CDCl_3$ with tetramethyl silane (TMS) as the internal reference. Infrared (IR) spectra were recorded on a Shimadzu IR Affinity-1 FTIR spectrophotometer with the DRS-8000A accessory and reported in cm^{-1}. Utilizing a Waters Q-TOF (ESI–MS) system, mass spectra were obtained. All spectral analyses, including mass and NMR spectrometry, were carried out at Punjab University's Sophisticated Analytical Instrument Facility (SAIF) in Chandigarh, India.

Synthesis of Substituted Flavanone, Hesperidin, and Hesperidin Arylhydrazones

Substituted arylhydrazones of flavanone were synthesized via a condensation reaction with substituted phenylhydrazines. Equimolar quantities (5 mmol) of each flavanone and the respective substituted phenylhydrazine were dissolved in ethanol (50 mL) with a catalytic amount of acetic acid (0.5 mL). The reaction mixtures were refluxed for appropriate durations, 6 to 17 hours for flavanone derivatives. After cooling to ambient temperature, the obtained precipitates were isolated by vacuum filtration and purified by rinsing with ethanol.

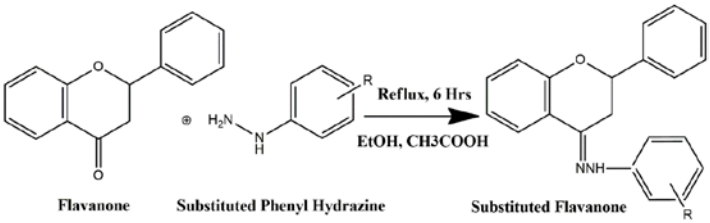

Scheme1: Synthesis of Flavanone Derivatives

Characterization data of synthesized flavanone derivatives

Compound 1: IR (KBr) ν (cm^{-1}): 3010 (Ar=C–H stretching), 1610 (C=N stretching), 1589 (C–C stretching), 1592, 1462, 1419 (Ar C=C stretching), 1190 (C–O–C stretching), 1506 (NO_2 stretching); ^{1}H NMR (DMSO-d_6) δ (ppm): 2.78–2.92 (m, 1H, H-3a), 3.36–3.48 (m, 1H, H-3b), 5.28 (dd, 1H, J = 12.2, 3.1 Hz, H-2), 6.98 (d, 1H, J = 8.2 Hz, H-8), 7.08 (t, 1H, J = 7.8 Hz, H-7), 7.32 (t, 1H, J = 7.6 Hz, H-6), 7.45–7.62 (m, 3H, Ar-H), 7.85 (d, 1H, J = 8.6 Hz), 8.12 (dd, 1H, J = 8.6, 2.2 Hz), 8.28 (d, 1H, J = 2.2 Hz), 8.41 (d, 1H, J = 8.8 Hz), 10.42 (s, 1H, NH); HRMS (ESI-QTOF): m/z calculated for $C_{21}H_{16}N_4O_5$ $[M+H]^+$ = 404.1090, found = 404.1085;Elemental analysis: C, 62.37; H, 3.99; N, 13.86; O, 19.78.

Compound 2: IR (KBr) ν (cm^{-1}): 3012 (Ar=C–H stretching), 1667 (C=N stretching), 1598 (C–C stretching), 1567, 1485, 1443 (Ar C=C stretching), 1178 (C–O–C stretching), 1506 (NO_2 stretching); ^{1}H NMR (DMSO-d_6) δ (ppm): 2.76–2.88 (m, 1H, H-3a), 3.34–3.44 (m, 1H, H-3b), 5.24 (dd, 1H, J = 12.0, 3.0 Hz, H-2), 6.94 (d, 1H, J = 8.0 Hz), 7.01 (t, 1H, J = 7.6 Hz), 7.26 (t, 1H, J = 7.6 Hz), 7.36–7.48 (m, 4H, Ar-H), 7.58 (d, 2H, J = 8.4 Hz),

7.82 (d, 2H, J = 8.4 Hz), 10.26 (s, 1H, NH).; HRMS (ESI-QTOF): m/z calculated for $C_{21}H_{17}ClN_2O$ $[M+H]^+$ = 349.1102, found = 349.1098; Elemental analysis: C, 72.31; H, 4.91; Cl, 10.16; N, 8.03; O, 4.59.

Compound 3: IR (KBr) ν (cm^{-1}): 3065 (Ar=C–H stretching), 2840 (C=N stretching), 1658 (C=O stretching), 1600 (C–C stretching), 1559, 1458, 1420 (Ar C=C stretching), 1196 (C–O–C stretching), 1124 (C–O stretching), 757 (C–Cl stretching); ^{1}H NMR (DMSO-d_6) δ (ppm): 2.79–2.91 (m, 1H, H-3a), 3.38–3.49 (m, 1H, H-3b), 5.29 (dd, 1H, J = 12.1, 3.2 Hz, H-2), 6.97 (d, 1H, J = 8.1 Hz), 7.06 (t, 1H, J = 7.8 Hz), 7.30 (t, 1H, J = 7.6 Hz), 7.42–7.55 (m, 3H), 7.90 (d, 2H, J = 8.8 Hz), 8.18 (d, 2H, J = 8.8 Hz), 10.38 (s, 1H, NH).; HRMS (ESI-QTOF): m/z calculated for $C_{21}H_{17}N_3O_3$ $[M+H]^+$ = 360.1343, found = 360.1338; Elemental analysis calculated for $C_{21}H_{17}N_3O_3$: C, 70.18; H, 4.77; N, 11.69. Found: C, 70.05; H, 4.71; N, 11.60.

Compound 4: IR (KBr) ν (cm^{-1}): 3200 (O–H stretching), 3117 (Ar=C–H stretching), 1670 (C=N stretching), 1612 (C–C stretching), 1576, 1456, 1426 (Ar C=C stretching), 1488 (N–O asymmetric stretching), 1369 (N–O symmetric stretching), 1167 (C–O–C stretching); ^{1}H NMR (DMSO-d_6) δ (ppm): 2.75–2.86 (m, 1H, H-3a), 3.32–3.42 (m, 1H, H-3b), 5.22 (dd, 1H, J = 12.0, 3.0 Hz, H-2), 6.91 (d, 1H, J = 8.0 Hz), 6.99 (t, 1H, J = 7.6 Hz), 7.23 (t, 1H, J = 7.6 Hz), 7.30–7.52 (m, 8H, Ar-H), 7.65 (d, 2H, J = 7.6 Hz), 10.21 (s, 1H, NH); HRMS (ESI-QTOF): m/z calculated for $C_{22}H_{20}N_2O$ $[M+H]^+$ = 329.1598, found = 329.1591; Elemental analysis: calculated C, 80.46; H, 6.14; N, 8.53; O, 4.87; found C, 80.21; H, 6.09; N, 8.47.

Compound 5: IR (KBr) ν (cm^{-1}): 3342 (O–H stretching), 3038 (Ar=C–H stretching), 1669 (C=N stretching), 1587 (C–C stretching), 1553, 1460, 1432 (Ar C=C stretching), 1214 (C–O stretching), 1117 (C–O–C stretching), 1499 (NO_2 stretching); ^{1}H NMR (DMSO-d_6) δ (ppm): 2.80–2.93 (m, 1H, H-3a), 3.39–3.50 (m, 1H, H-3b), 5.30 (dd, 1H, J = 12.2, 3.1 Hz, H-2), 6.99 (d, 1H, J = 8.0 Hz), 7.09 (t, 1H, J = 7.8 Hz), 7.34 (t, 1H, J = 7.6 Hz), 7.46–7.60 (m, 3H), 7.78 (t, 1H, J = 7.8 Hz), 8.05 (d, 1H, J = 8.2 Hz), 8.22 (dd, 1H, J = 8.2, 2.0 Hz), 8.36 (s, 1H), 10.45 (s, 1H, NH); HRMS (ESI-QTOF): m/z calculated for $C_{21}H_{17}N_3O_3$ $[M+H]^+$ = 360.1343, found = 360.1338; Elemental analysis: calculated C, 70.18; H, 4.77; N, 11.69; O, 13.36; found C, 70.05; H, 4.71; N, 11.60.

Compound 6: IR (KBr) ν (cm^{-1}): 3342 (O–H stretching), 3038 (Ar=C–H stretching), 2846 (C=N stretching), 1669 (C=O stretching), 1587 (C–C stretching), 1553, 1460, 1432 (Ar C=C stretching), 1214 (C–O stretching), 1117 (C–O–C stretching), 1234 (C–F stretching); ^{1}H NMR (DMSO-d_6) δ (ppm): 2.76–2.88 (m, 1H, H-3a), 3.35–3.46 (m, 1H, H-3b), 5.25 (dd, 1H, J = 12.1, 3.1 Hz, H-2), 6.95 (d, 1H, J = 8.0 Hz), 7.02 (t, 1H, J = 7.6 Hz), 7.26 (t, 1H, J = 7.6 Hz), 7.34–7.46 (m, 3H), 7.12–7.20 (m, 2H, Ar–F), 7.58 (dd, 2H, J = 8.4, 5.6 Hz), 10.27 (s, 1H, NH); HRMS (ESI-QTOF): m/z calculated for $C_{21}H_{17}FN_2O$ $[M+H]^+$ = 333.1291, found = 333.1286;Elemental analysis: C, 75.89; H, 5.16; F, 5.72; N, 8.43; O, 4.81.

Compound 7: IR (KBr) ν (cm^{-1}): 3342 (O–H stretching), 3038 (Ar=C–H stretching), 2846 (C=N stretching), 1669 (C=O stretching), 1587 (C–C stretching), 1553, 1460, 1432 (Ar C=C stretching), 1214 (C–O stretching), 1117 (C–O–C stretching), 638 (C–Br stretching); ^{1}H NMR (DMSO-d_6) δ (ppm): 2.77–2.89 (m, 1H, H-3a), 3.36–3.47 (m, 1H, H-3b), 5.26 (dd, 1H, J = 12.0, 3.1 Hz, H-2), 6.95 (d, 1H, J = 8.0 Hz), 7.03 (t, 1H, J = 7.6 Hz), 7.28 (t, 1H, J = 7.6 Hz), 7.36–7.50 (m, 3H), 7.62 (d, 2H, J = 8.4 Hz), 7.78 (d, 2H, J = 8.4 Hz), 10.30 (s, 1H, NH); HRMS (ESI-QTOF): m/z calculated for $C_{21}H_{17}BrN_2O$ $[M+H]^+$ = 393.0497, found = 393.0492;Elemental analysis: C, 64.13; H, 4.36; Br, 20.32; N, 7.12; O, 4.07.

Compound 8: IR (KBr) ν (cm^{-1}): 3342 (O–H stretching), 3038 (Ar=C–H stretching), 2846 (C=N stretching), 1669 (C=O stretching), 1587 (C–C stretching), 1553, 1460, 1432 (Ar C=C stretching), 1214 (C–O stretching), 1117 (C–O–C stretching), 2830 (OCH_3 stretching); ^{1}H NMR (DMSO-d_6) δ (ppm): 2.68–2.82 (m, 1H, H-3a), 3.30–3.42 (m, 1H, H-3b), 3.74 (s, 3H, OCH_3), 5.23 (dd, 1H, J = 12.0, 3.0 Hz, H-2), 6.82 (d, 1H, J = 8.0 Hz), 6.90 (t, 1H, J = 7.6 Hz), 7.15 (t, 1H, J = 7.6 Hz), 6.95–7.10 (m, 3H), 7.30–7.48 (m, 3H), 10.18 (s, 1H, NH); HRMS (ESI-QTOF): m/z calculated for $C_{22}H_{20}N_2O_2$ $[M+H]^+$ = 345.1598, found = 345.1592; Elemental analysis calculated for $C_{22}H_{20}N_2O_2$: C, 76.72; H, 5.85; N, 8.13. Found: C, 76.55; H, 5.78; N, 8.04.

Compound 9: IR (KBr) ν (cm^{-1}): 3342 (O–H stretching), 3038 (Ar=C–H stretching), 2846 (C=N stretching), 1669 (C=O stretching), 1587 (C–C stretching), 1553, 1460, 1432 (Ar C=C stretching), 1214 (C–O stretching), 1117 (C–O–C stretching), 2830 ($C–CH_3$ stretching); ^{1}H NMR (DMSO-d_6) δ (ppm): 2.32 (s,

3H, CH_3), 2.74–2.86 (m, 1H, H-3a), 3.33–3.44 (m, 1H, H-3b), 5.22 (dd, 1H, J = 12.0, 3.0 Hz, H-2), 6.88 (d, 1H, J = 8.0 Hz), 6.96 (t, 1H, J = 7.6 Hz), 7.20 (t, 1H, J = 7.6 Hz), 7.10–7.35 (m, 6H), 7.42 (d, 1H, J = 7.6 Hz), 10.15 (s, 1H, NH); HRMS (ESI-QTOF): m/z calculated for $C_{22}H_{20}N_2O$ $[M+H]^+$ = 329.1598, found = 329.1593; Elemental analysis calculated for $C_{22}H_{20}N_2O$: C, 80.46; H, 6.14; N, 8.53. Found: C, 80.28; H, 6.07; N, 8.45.

ANTICANCER EVALUATION OF THE SYNTHESIZED DERIVATIVES

In Vitro Anti-breast Cancer Activity Evaluation against MCF-7 and MDA-MB-231 Cell Lines

The synthesized test compounds were evaluated for in vitro anticancer activity against two breast cancer cell lines: MCF-7 (hormone-dependent) and MDA-MB-231 (triple-negative). These cell lines were selected because of their clinical relevance and widespread use as experimental models in breast cancer research. All experiments were performed in triplicate at each concentration to ensure reproducibility and statistical reliability. The cytotoxic potential of the synthesized compounds was assessed using the colorimetric MTT assay, a well-established method for determining cell viability based on the reduction of MTT to insoluble formazan crystals by metabolically active cells. The amount of formazan formed was quantified spectrophotometrically and used as an indicator of viable cell number following treatment. Tamoxifen, a clinically established anticancer agent, was used as the positive control to provide a benchmark for comparing the activity of the synthesized derivatives under identical experimental conditions.

The anticancer activity of the compounds was evaluated by calculating the percentage of cell growth inhibition at different concentrations. Furthermore, the half-maximal inhibitory concentration (IC_{50}) values were determined for each compound, representing the concentration required to inhibit 50% of cell growth and serving as an important parameter for comparing the cytotoxic potency of the tested compounds.

Methodology

The cytotoxic activity of the synthesized flavanone–arylhydrazone derivatives was evaluated against MCF-7 and MDA-MB-231 breast cancer cell lines using the MTT assay. Cells (1×10^4 cells/well) were seeded into 96-well plates and allowed to attach under standard culture conditions [35-36]. The cells were then treated with the synthesized test compounds at different concentrations ranging from 50 to 250 µM to generate dose–response curves and determine IC_{50} values. Following incubation at 37 °C in a humidified CO_2 incubator, 10 µL of MTT solution (5 mg/mL in PBS) was added to each well and incubated for an additional 4 h. The resulting formazan crystals were dissolved in 100 µL dimethyl sulfoxide (DMSO), and absorbance was measured at 490 nm using a microplate reader (Model 680, Bio-Rad, USA). Cell viability was expressed as a percentage relative to untreated control cells. The percentage growth inhibition and half-maximal inhibitory concentration (IC_{50}) values were calculated from the dose–response curves using GraphPad Prism software.

RESULT

Chemistry

A novel series of flavanone-based arylhydrazone derivatives (1–9) was successfully synthesized via condensation of substituted flavanones with substituted phenylhydrazines under reflux conditions in ethanol using a catalytic amount of acetic acid. The reaction proceeded smoothly, affording the desired products in moderate to good yields (63–85%). The synthesized compounds were purified by filtration followed by recrystallization Table 1. The IR spectra of the synthesized flavanone–arylhydrazone derivatives showed characteristic absorption bands in the region of 1600–1669 cm^{-1}, corresponding to the azomethine (C=N) group and supporting the formation of the desired hydrazone derivatives. In several compounds, absorption bands attributable to the flavanone carbonyl group were also observed, indicating that the ketone functionality remained intact in the final structures.

The presence of these characteristic bands, along with the expected aromatic & heterocyclic vibrations, further confirmed the successful synthesis of the target compounds. Additionally, N–H stretching vibrations were observed in the region of 3300–3400 cm^{-1}, consistent with the hydrazone moiety. The ^1H NMR spectra of all compounds showed characteristic signals corresponding to the flavanone scaffold. The methine proton at C-2 appeared as a doublet of doublets in the region of δ 5.20–5.30 ppm (J ≈ 12.0 and 3.0 Hz), while the diastereotopic methylene protons at C-3 were observed as multiplets in the range of δ 2.70–3.50 ppm.

A distinct singlet corresponding to the hydrazone –NH proton was consistently observed in the downfield region (δ 10.15–10.45 ppm), confirming the formation of the hydrazone functionality. Importantly, the aromatic region (δ ~6.80–8.50

ppm) displayed clear substituent-dependent variations across the series. Compounds bearing electron-withdrawing groups (e.g., nitro and halogens) exhibited relatively downfield shifts, whereas electron-donating substituents (e.g., methoxy and methyl) showed comparatively upfield signals. Substituent-specific signals such as methoxy (–OCH_3) and methyl (–CH_3) protons were observed at their expected chemical shift regions.

These observations confirm the structural diversity of the synthesized derivative & address earlier inconsistencies in spectral reporting. Further structural confirmation was obtained from HRMS (ESI-QTOF) analysis, which showed molecular ion peaks $[M+H]^+$ in excellent agreement with the calculated exact masses for all compounds, thereby validating their molecular formulas with high accuracy. Scheme 1 illustrates the synthetic strategy for the preparation of flavanone-arylhydrazone derivatives.

The reaction involved equimolar amounts of flavanone (5 mmol) and substituted phenylhydrazines in refluxing ethanol (50 mL) with a catalytic amount of acetic acid (0.5 mL) for 6–17 hours. Upon completion, the reaction mixtures were cooled to room temperature, and the resulting precipitates were isolated by vacuum filtration and purified by washing with ethanol. The physicochemical properties of the synthesized compounds are summarized in Table 1, while the substituent pattern is presented in Table 2, facilitating correlation between structural features and biological activity.

Table 1. Physicochemical properties of synthesized flavanone-arylhydrazone derivatives

SN	Compound	Substituent (R)	Molecular Formula	Molecular Weight	Yield (%)	M.P. (°C)	Rf Value*
1	Compound 1	2,4-NO_2	$C_{21}H_{16}N_4O_5$	404.38(g/mol)	78	197–199	0.77
2	Compound 2	4-Cl	$C_{21}H_{17}ClN_2O$	348.83(g/mol)	73	241–243	0.59
3	Compound 3	4-NO_2	$C_{21}H_{17}N_3O_3$	359.38(g/mol)	85	238–242	0.74
4	Compound 4	4-Phenyl	$C_{22}H_{20}N_2O$	328.41(g/mol)	80	115–120	0.82
5	Compound 5	3-NO_2	$C_{21}H_{17}N_3O_3$	359.38(g/mol)	65	217–218	0.68
6	Compound 6	4-F	$C_{21}H_{17}FN_2O$	332.37(g/mol)	63	258–259	0.81
7	Compound 7	4-Br	$C_{21}H_{17}BrN_2O$	393.28(g/mol)	79	197–199	0.77
8	Compound 8	3-OCH_3	$C_{22}H_{20}N_2O_2$	344.41(g/mol)	73	150–151	0.59
9	Compound 9	2-CH_3	$C_{22}H_{20}N_2O$	328.41(g/mol)	69	165–168	0.78

Rf values determined using ethyl acetate: formic acid: water (8:1:1)

Table 2: Substituent Pattern of Synthesized Flavanone-Arylhydrazone Derivatives

Compound No.	Substituent (R)	Type of Substituent	Electronic Nature
1	2,4-NO_2	Dinitro	Strong EWG
2	4-Cl	Chloro	Moderate EWG
3	4-NO_2	Nitro	Strong EWG
4	4-Phenyl	Phenyl	Weak EDG / hydrophobic
5	3-NO_2	Nitro	Strong EWG
6	4-F	Fluoro	Moderate EWG
7	4-Br	Bromo	Moderate EWG
8	3-OCH_3	Methoxy	EDG
9	2-CH_3	Methyl	EDG

This information is already derivable from your Table 1 (R column) but reorganized for clarity

ANTICANCER ACTIVITY

The synthesized flavanone-arylhydrazone derivatives, identified as compounds 1 to 9, were subjected to comprehensive in vitro evaluation for their anti-breast cancer efficacy using established whole-cell models, specifically the hormone-dependent MCF-7 line, which simulates estrogen receptor-positive luminal breast tumors responsive to endocrine therapy, and the aggressive triple-negative MDA-MB-231 line, indicative of clinically resistant cases marked by rapid proliferation, epithelial-mesenchymal transition, and a propensity for metastasis due to dysregulated activation of survival pathways independent of canonical receptors. The assays precisely measured the percentage of viable cells after exposure to the test agents, comparing results to vehicle-treated controls to assess the extent of cytotoxicity and evaluate the compounds' ability to disrupt cellular homeostasis through various mechanisms, including membrane disruption, energy depletion, and the initiation of programmed cell death. Tamoxifen, the primary selective

estrogen receptor modulator (SERM) in the clinical arsenal for hormone-responsive breast cancers, served as the standard positive control, providing a reference for comparative potency and selectivity. Its mechanism relies on competitive antagonism of estrogen binding to ERα, recruitment of corepressors, and subsequent suppression of proliferative gene transcription, enabling direct comparison of the novel hybrids' receptor-independent actions against this targeted model.

Evaluations covered a broad concentration gradient, from submicromolar levels to significantly higher concentrations exceeding expected therapeutic ranges, facilitating thorough characterization of sigmoidal dose-response curves that reveal potency thresholds, maximum efficacy plateaus, and potential steepness suggestive of cooperative target engagement or allosteric modulation. Cell viability metrics were obtained at specific intervals across this spectrum, with inhibition percentages calculated relative to control baselines to account for inherent growth kinetics and media variability.

This resulted in graphical representations that plot inhibition levels against logarithmic concentration scales for both cell models, enabling visual and statistical evaluation of response profiles. The accompanying visualizations (Figure 1 for MCF-7 and Figure 2 for MDA-MB-231) demonstrate that all derivatives exhibited characteristic dose-dependent cytotoxicity profiles. Incremental dosing progressively diminished cell viability by increasingly obstructing metabolic function, as assessed by mitochondrial dehydrogenase activity in the colorimetric readout. Significant inhibition was observed at elevated exposures, which corresponded with the saturation of cellular repair and adaptation mechanisms.

This behavior highlights the hybrids' involvement in concentration-dependent pharmacodynamics, likely amplifying initial receptor-ligand interactions through subsequent pathways involving kinase cascades, proteasomal overload, or lysosomal destabilization. The varying slopes and midpoints among cell lines suggested subtype-specific vulnerabilities, with MCF-7 showing moderate responsiveness linked to hormonal circuit disruptions, in contrast to MDA-MB-231's sharper declines indicative of metabolic rigidity in nutrient-deficient microenvironments.

These patterns not only validate the scaffold's adaptability across breast cancer heterogeneity but also highlight structural motifs that enhance control performance, facilitating predictive modeling for clinical extrapolations, resistance forecasting through serial passage experiments, and synergistic combinations with radiation or immunotherapies to leverage synthetic lethality in polygenic tumor contexts, thus augmenting the preclinical dataset for informed lead triaging in oncology pipelines.

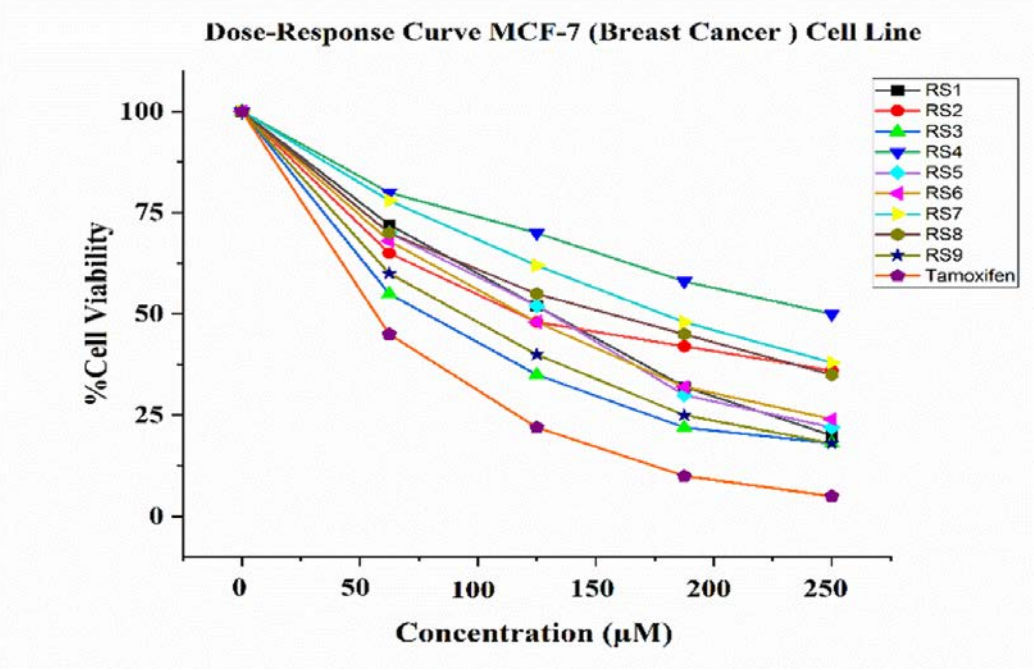

Figure 1: High-resolution dose–response curves showing the effect of synthesized flavanone-arylhydrazone derivatives on MCF-7 breast cancer cells.

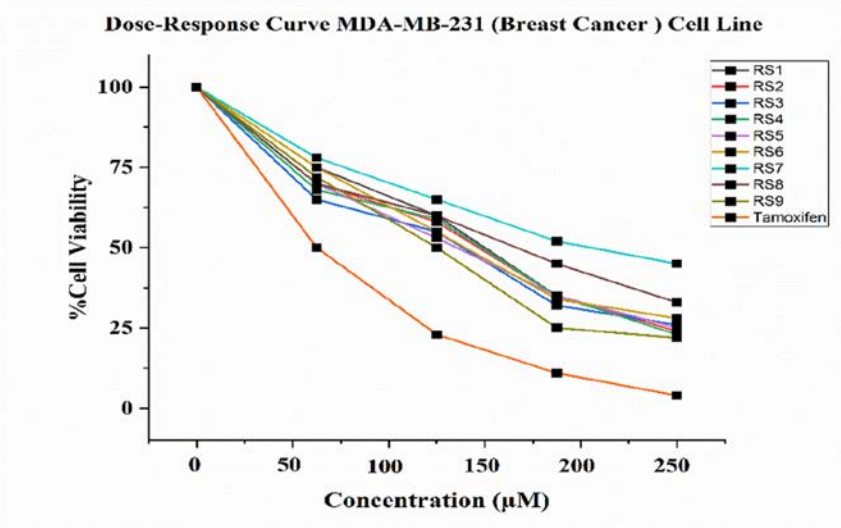

Figure 2: High-resolution dose–response curves showing the effect of synthesized flavanone-arylhydrazone derivatives on MDA-MB-231 breast cancer cells

Comparison with standard tamoxifen showed that it had the lowest IC_{50} values of 11.46 ± 0.2 µM (MCF-7) & 27.13 ± 0.4 µM (MDA-MB-231), indicating strong cytotoxic activity. The IC_{50} values of the synthesized compounds against MCF-7 & MDA-MB-231 cell lines are summarized in Table 3. In contrast, all tested compounds exhibited higher IC_{50} values, reflecting lower potency. Nevertheless, compounds 1, 3, 5 & 6 demonstrated the most consistent cytotoxic activity across both breast cancer cell lines. Although Compound 9 showed moderate activity against MCF-7 cells (IC_{50} = 65.45 ± 4.5 µM), its substantially weaker activity against MDA-MB-231 cells (IC_{50} = 195.69 ± 5.49 µM) suggests a cell line-selective rather than broad-spectrum cytotoxic profile.

Table 3: IC_{50} Values of Synthesized Compounds Against Breast Cancer Cell Lines

S. No.	Molecule	IC_{50} (µM) – MCF-7	IC_{50} (µM) – MDA-MB-231
1	Compound 1	36.6 ± 2.4	44.21 ± 2.7
2	Compound 2	145.1 ± 5.4	125.02 ± 8.4
3	Compound 3	33.54 ± 2.2	41.08 ± 2.6
4	Compound 4	206.18 ± 9.75	241.13 ± 5.85
5	Compound 5	60.42 ± 4.3	89.53 ± 3.6
6	Compound 6	72.11 ± 3.2	59.98 ± 4.2
7	Compound 7	259.80 ± 7.99	159.76 ± 9.74
8	Compound 8	173.40 ± 5.78	294.84 ± 9.04
9	Compound 9	65.45 ± 4.5	195.69 ± 5.49
10	Tamoxifen (Standard)	11.46 ± 0.2	27.13 ± 0.4

"Compound 3 demonstrated the lowest IC_{50} among the synthesized derivatives, indicating superior cytotoxic potency. "Values expressed as mean ± SD (n = 3).

Comparison between MCF-7 & MDA-MB-231 Cytotoxicity

In this study, the synthesized compounds showed various levels of cytotoxicity against MCF-7 and MDA-MB-231 cell lines derived from breast cancer, suggesting potential differences in their mechanisms of action, receptor interactions, and cellular uptake. Notably, Compounds 3, 1, 5, and 6 demonstrated comparable cytotoxicity across both cell lines, indicating their potential as broad-spectrum anticancer agents. In contrast, Compound 9 displayed marked selectivity toward MCF-7 cells and substantially reduced potency against MDA-MB-231 cells, indicating that its activity is not broad-spectrum.

Structure-Activity Relationship

The structure-activity relationship analysis offers explanations for the molecular features contributing to cytotoxicity. Compounds bearing electron-withdrawing functional groups, such as halogens, nitro, and carbonyl moieties, appeared to enhance anticancer activity, likely due to their influence on electron density and molecular interactions with cellular targets. Furthermore, the presence of hydrophobic moieties may play a crucial role in membrane permeability, particularly in MDA-MB-231 cells, which lack estrogen receptor expression and rely on alternative pathways for drug uptake. The SAR analysis

suggests that compounds with electron-withdrawing functional groups (e.g., halogens, nitro, carbonyl) might contribute to enhanced activity. The presence of hydrophobic moieties could influence membrane permeability. This was especially observed in the triple-negative MDA-MB-231 cell line. The observed differences in potency between ER-positive and triple-negative breast cancer cells could be due to variations in estrogen receptor interactions, apoptotic signaling, and drug efflux processes. These results emphasize the significance of molecular modifications in optimizing the cytotoxic potential of these compounds and warrant further investigation into their mechanistic pathways and therapeutic applicability.

DISCUSSION

Biological evaluation revealed that all compounds exhibited dose-dependent cytotoxicity in both breast cancer cell lines [12]. Among the series, compounds bearing electron-withdrawing substituents, particularly nitro and halogen groups, demonstrated relatively enhanced cytotoxic activity [13]. Compounds 3 and 1 showed the lowest IC_{50} values, indicating comparatively higher potency within the synthesized series[14]. However, the observed differences in activity among derivatives were modest, suggesting that electronic effects alone do not fully account for the structure–activity relationship (SAR). Other physicochemical factors, such as lipophilicity, steric effects, and cellular permeability, are likely to contribute significantly to the observed biological activity [15]. For example, halogen substituents may enhance membrane permeability due to increased lipophilicity, potentially compensating for their comparatively weaker electron-withdrawing nature[16].

Despite incorporating two pharmacologically relevant motifs, namely the flavanone scaffold and the arylhydrazone pharmacophore, the synthesized hybrids displayed only moderate cytotoxic potency compared with tamoxifen [17]. One possible explanation is that the arylhydrazone moiety increases molecular size and conformational flexibility, thereby reducing the molecules' ability to adopt an optimal binding orientation at their intracellular targets [18]. The relatively moderate cytotoxic potency and comparatively high IC_{50} values observed in the present study may also be influenced by the exposure duration used during the MTT assay. The objective of employing shorter treatment periods was to evaluate the early cellular response to the synthesized compounds. However, conventional anticancer screening protocols commonly utilize 48–72 h incubation periods, allowing multiple cell-doubling cycles and prolonged drug exposure, which often results in greater growth inhibition and lower IC_{50} values. Therefore, the IC_{50} values reported in the present study should be interpreted within the context of the selected incubation period. Future investigations employing longer exposure times are warranted to provide a more comprehensive assessment of the antiproliferative potential of these flavanone–arylhydrazone derivatives [19].

In addition, the hydrazone linkage introduces additional hydrogen-bond donor and acceptor functionalities that can alter the overall physicochemical profile of the compounds. Although a certain degree of lipophilicity is beneficial for membrane permeation, excessive steric bulk and increased molecular complexity may hinder efficient cellular uptake or limit access to target binding sites. This could explain why compounds with different substituents exhibited only modest variations in activity despite noticeable electronic differences [20].

Furthermore, unlike tamoxifen, which acts through a well-defined and highly optimized interaction with estrogen receptors, the synthesized derivatives may exert their effects through less specific or multiple cellular mechanisms, resulting in comparatively higher IC_{50} values [21].

The relatively moderate cytotoxic potency and comparatively high IC_{50} values observed in the present study may also be influenced by the exposure duration used during the MTT assay. The objective of employing shorter treatment periods was to evaluate the early cellular response to the synthesized compounds. However, conventional anticancer screening protocols commonly utilize 48–72 h incubation periods, allowing multiple cell-doubling cycles and prolonged drug exposure, which often results in greater growth inhibition and lower IC_{50} values. Therefore, the IC_{50} values reported in the present study should be interpreted within the context of the selected incubation period. Future investigations employing longer exposure times are warranted to provide a more comprehensive assessment of the antiproliferative potential of these flavanone–arylhydrazone derivatives [22]. Therefore, future structural optimization should focus on achieving a better balance between molecular size, lipophilicity, cellular permeability, and target affinity to improve anticancer potency. The current study is limited to cytotoxicity evaluation using the MTT assay [23], which primarily reflects metabolic activity and

does not provide mechanistic insights into cell death pathways [24]. Therefore, the precise molecular mechanisms underlying the observed anticancer effects remain unclear[25]. Future studies involving apoptosis assays, cell cycle analysis, and molecular target identification will be necessary to elucidate the mode of action.

CONCLUSION

In conclusion, the present study reports the successful synthesis and characterization of a series of novel flavanone-arylhydrazone derivatives and their evaluation for in vitro anticancer activity against MCF-7 and MDA-MB-231 breast cancer cell lines. The synthesized compounds demonstrated dose-dependent cytotoxicity, with several derivatives, particularly compounds 3 and 1, exhibiting moderate activity across both cell models. Structure–activity relationship analysis indicated that the presence of electron-withdrawing substituents, such as nitro and halogen groups, may contribute to enhanced cytotoxic effects, possibly by modulating physicochemical properties such as lipophilicity and cellular permeability. However, no clear linear correlation between electronic effects and biological activity was observed, suggesting that multiple structural factors influence the overall activity profile. Although the compounds showed promising cytotoxic potential, their potency remained lower than that of the reference drug tamoxifen, highlighting the need for further structural optimization. Importantly, the current findings are based solely on cell viability assays and do not provide direct insight into the underlying molecular mechanisms of action. Therefore, the proposed involvement of specific pathways or receptor-independent mechanisms remains speculative and requires validation through detailed mechanistic studies. Future investigations involving apoptosis assays, cell cycle analysis, and molecular target identification will be essential to elucidate the mode of action & therapeutic relevance of these compounds. Overall, flavanone-arylhydrazone hybrids represent a promising scaffold for further development, and the present study provides a foundation for continued optimization and mechanistic exploration toward potential anticancer applications.

FINANCIAL ASSISTANCE

NIL

CONFLICT OF INTEREST

The authors declare no conflict of interest.

AUTHOR CONTRIBUTION

Reena Singh conceptualized and designed the study, conducted the experimental work, performed data acquisition and analysis, and drafted the manuscript. Yogesh Murti provided supervision throughout the research process, contributed to the study design and data interpretation, and critically revised the manuscript for important intellectual content. Both authors read and approved the final version of the manuscript.

DECLARATION OF USE OF AI TOOLS

The authors used QuillBot solely for grammar correction and paraphrasing to improve the readability and language of the manuscript. All scientific content, data analysis, interpretations, and conclusions are the original work of the authors. The authors reviewed and verified the final manuscript and take full responsibility for its originality, accuracy, and integrity.

REFERENCES

[1] Kopustinskiene DM, Jakstas V, Savickas A, Bernatoniene J. Flavonoids as anticancer agents. *Nutrients,* **12**, 457 (2020) https://doi.org/10.3390/nu12020457

[2] Yang C, Gong Q, Zhu R, Fan Y, Wang Q, Ge G, et al. Flavonoids as promising drug leads: structural diversity, synthetic strategies, and drug-likeness optimization. *Eur J Med Chem,* **305**, 118549 (2026) https://doi.org/10.1016/j.ejmech.2025.118549

[3] Charan S, Maksud N, Gupta A, Devi S, Alam MM, Akhter M, et al. Anticancer activity of hydrazones in the last quinquennial period: a special emphasis on various enzyme targets and SAR. *Eur J Med Chem,* **302**, 118305 (2026) https://doi.org/10.1016/j.ejmech.2025.118305

[4] Hossain MS, Wazed MA, Asha S, Amin MR, Shimul IM. Dietary phytochemicals in health and disease: mechanisms, clinical evidence, and applications — a comprehensive review. *Food Sci Nutr,* **13**, e70101 (2025) https://doi.org/10.1002/fsn3.70101

[5] Aljohani MS, Hu X. Molecular recognition of diaryl ureas in their targeted proteins — a data mining and quantum chemical study. *Molecules,* **30**, 1007 (2025) https://doi.org/10.3390/molecules30051007

[6] Kerru N, Singh P, Koorbanally N, Raj R, Kumar V. Recent advances (2015–2016) in anticancer hybrids. *Eur J Med Chem,* **142**, 179–212 (2017) https://doi.org/10.1016/j.ejmech.2017.07.033

[7] Tafere DA, Gebrezgiabher M, Elemo F, Sani T, Atisme TB, Ashebr TG, et al. Hydrazones, hydrazones-based coinage metal complexes, and their biological applications. *RSC Adv,* **15**, 6191 (2025) https://doi.org/10.1039/D4RA07794F

[8] Mala GA, Friedrich HB, Ibrahim H, Ndahi NP, Zamisa SJ, Masokano DSA, et al. The influence of halogen-substituted anisaldehyde and aminophenol precursors on the solid-state

molecular conformation and antiproliferative activity of resulting Schiff bases. *Bioorg Chem*, **163**, 108638 (2025) https://doi.org/10.1016/j.bioorg.2025.108638

[9] Jurj ED, Colibășanu D, Vasii SO, Suciu L, Dehelean CA, Udrescu L. Redefining breast cancer care by harnessing computational drug repositioning. *Medicina (B Aires)*, **61**, 1640 (2025) https://doi.org/10.3390/medicina61091640

[10] Kotyan S, Chandana SN, Ganesha DP, Lakshminarayana BN, Pandikatte N, Deb PK, et al. Synthesis of novel arylhydrazones bearing 8-trifluoromethyl quinoline: crystal insights, larvicidal activity, ADMET predictions, and molecular docking studies. *Pharmaceuticals*, **18**, 1804 (2025) https://doi.org/10.3390/ph18121804

[11] Abdullah MN, Abd Hamid S, Muhamad Salhimi S, Jalil NAS, Al-Amin M, Jumali NS. Design and synthesis of 1-sec/tert-butyl-2-chloro/nitrophenylbenzimidazole derivatives: molecular docking and in vitro evaluation against MDA-MB-231 and MCF-7 cell lines. *J Mol Struct*, **1277**, 134828 (2023) https://doi.org/10.1016/j.molstruc.2022.134828

[12] Zubrickė I, Jonuškienė I, Kantminienė K, Tumosienė I, Petrikaitė V. Synthesis and in vitro evaluation as potential anticancer and antioxidant agents of diphenylamine-pyrrolidin-2-one-hydrazone derivatives. *Int J Mol Sci*, **24**, 16804 (2023) https://doi.org/10.3390/ijms242316804

[13] Katariya KD, Shah SR, Reddy D. Anticancer, antimicrobial activities of quinoline based hydrazone analogues: synthesis, characterization and molecular docking. *Bioorg Chem*, **94**, 103406 (2020) https://doi.org/10.1016/j.bioorg.2019.103406

[14] Kulić Ž, Steiner VJN, Butterer A. NMR chemical shifts of common flavonoids. *Planta Med*, **92**, 58 (2025) https://doi.org/10.1055/a-2706-7473

[15] Géhin C, Holman SW. Advances in high-resolution mass spectrometry applied to pharmaceuticals in 2020: a whole new age of information. *Anal Sci Adv*, **2**, 142 (2021) https://doi.org/10.1002/ansa.202000149

[16] Bustos L, Echiburú-Chau C, Castro-Alvarez A, Bradshaw B, Simirgiotis MJ, Mellado M, et al. Cytotoxic effects on breast cancer cell lines of chalcones derived from a natural precursor and their molecular docking analysis. *Molecules*, **27**, 4387 (2022) https://doi.org/10.3390/molecules27144387

[17] Cherdtrakulkiat R, Boonpangrak S, Sinthupoom N, Prachayasittikul S, Ruchirawat S, Prachayasittikul V. Derivatives (halogen, nitro and amino) of 8-hydroxyquinoline with highly potent antimicrobial and antioxidant activities. *Biochem Biophys Rep*, **6**, 135 (2016) https://doi.org/10.1016/j.bbrep.2016.03.014

[18] Berrouet C, Dorilas N, Rejniak KA, Tuncer N. Comparison of drug inhibitory effects (IC50) in monolayer and spheroid cultures. *Bull Math Biol*, **82**, 68 (2020) https://doi.org/10.1007/s11538-020-00746-7

[19] Rathod NV, Mishra S. Synthesis, characterization and molecular docking study of novel bile acid curcumin conjugates as potent antibacterial and antibiofilm agents. *Sci Rep*, **15**, 34176 (2025) https://doi.org/10.1038/s41598-025-15297-x

[20] Nádaská D, Malík I. Insight into the in silico structural, physicochemical, pharmacokinetic and toxicological properties of antibacterially active viniferins and viniferin-based compounds as derivatives of resveratrol containing a (2,3-dihydro)benzo[b]furan privileged scaffold. *Appl Sci*, **15**, 8350 (2025) https://doi.org/10.3390/app15158350

[21] Molaei S, Shiran JA, Shakour N, Baradaran M, Malihi Z, Rahimi MR, et al. Synthesis of thiosemicarbazone Schiff base derivatives as anti-leishmanial agents and molecular dynamics simulations insights. *Sci Rep*, **15**, 24867 (2025) https://doi.org/10.1038/s41598-025-10545-6

[22] Valiathan C, McFaline JL, Samson LD. A rapid survival assay to measure drug-induced cytotoxicity and cell cycle effects. *DNA Repair (Amst)*, **11**, 92 (2011) https://doi.org/10.1016/j.dnarep.2011.11.002

[23] El Omari N, Khalid A, Makeen HA, Alhazmi HA, Albratty M, Mohan S, et al. Stochasticity of anticancer mechanisms underlying clinical effectiveness of vorinostat. *Heliyon*, **10**, e33052 (2024) https://doi.org/10.1016/j.heliyon.2024.e33052

[24] Haneen DSA, Abdalha AA, Alkhatib MM, Kamal M, Youssef ASA, Abou-Elmagd WSI, et al. Synthesis, comprehensive in silico studies, and cytotoxicity evaluation of novel quinazolinone derivatives as potential anticancer agents. *Sci Rep*, **15**, 23697 (2025) https://doi.org/10.1038/s41598-025-08062-7

[25] Zhuo Y, Zhao YG, Zhang Y. Enhancing drug solubility, bioavailability, and targeted therapeutic applications through magnetic nanoparticles. *Molecules*, **29**, 4854 (2024) https://doi.org/10.3390/molecules29204854